[16] Slattery, R. E. and Clay, W. G., "The turbulent wake of hypersonic bodies," ARS Preprint 2673-62 (1962).

[17] Lykoudis, P. S., "The growth of the hypersonic turbulent wake behind blunt and slender bodies," The Rand Corp. Memo. RM-3270-PR (January 1963).

[18] Pallone, A. J., Erdos, I. I., Eckerman, J., and McKay, W., "Hypersonic laminar wakes and transition studies," AIAA Preprint 63-171 (1963).

[19] Lees, L., "Hypersonic wakes and trails," ARS Preprint 2662-62 (1962).

[20] Demetriades, A. and Gold, H., "Transition to turbulence in the hypersonic wake of blunt-bluff bodies," ARS J. **32**, 1420–1421 (1962).

[21] Demetriades, A. and Gold, H., "Correlation of blunt-bluff body wake transition data," Graduate Aeronautical Lab., California Institute of Technology Internal Memo. 12 (September 1962).

NOVEMBER 1964 AIAA JOURNAL VOL. 2, NO. 11

A Theoretical Study of the Inviscid Hypersonic Flow about a Conical Flat-Top Wing-Body Combination

PAUL MANDL*
National Research Council, Ottawa, Ontario, Canada

By combining the theory of linearized characteristics with the hypersonic small disturbance approximation, explicit expressions are derived for the shock shape, the flow field, the surface pressure distribution, and the aerodynamic forces for a delta wing and half-cone combination traveling at hypersonic speeds and small incidence. The theory is applied to a particular configuration for which surface pressure measurements are available. The theoretical and experimental pressure distributions agree quite closely on the body surface; but in the wing-body junction and on the wing, the theory predicts pressures that are too low.

Nomenclature

a = local speed of sound
b = total wing span
C_A = axial force coefficient
C_D = drag coefficient
C_L = lift coefficient
C_N = normal force coefficient
C_p = pressure coefficient $[(p - p_\infty)/\frac{1}{2}\rho_\infty U_\infty^2]$
c_v = specific heat at constant volume
$g_{2n}, h_{2n}, j_{2n}, k_{2n}$ = Fourier coefficients
l = spanwise distance measured from windward generator
M_∞ = freestream Mach number
M_2 = flow Mach number perpendicular to leading edge
$\mathbf{n}$ = vector normal to shock surface
p = absolute pressure
$\mathbf{q}$ = fluid velocity vector
q = magnitude of fluid velocity
$\hat{q}$ = limit speed
R, θ, ϕ = spherical coordinates (Fig. 1)
S = specific entropy
s = nondimensional entropy
U_∞ = freestream velocity
u_{2n}, v_{2n}, w_{2n} = Fourier coefficient associated with fluid velocity
s_{2n} = Fourier coefficient associated with entropy distribution
α = incidence of configuration axis
γ = ratio of specific heats
δ = angle between shock normal and meridian plane
ϵ = density ratio across cone shock
θ_c = semiapex angle of cone
θ_s = local shock wave angle
λ = semiapex angle of wing
ρ = density
χ, = shock angle (Fig. 3)
χ' = angle between velocity perpendicular to leading edge and leading edge shock

Subscripts and Superscripts

∞ = freestream
e = region downstream of leading edge shock
0 = axially symmetric flow
b = body
w = wing

Received January 29, 1964; revision received May 28, 1964. A more detailed account of this research including further results is given in the National Aeronautical Establishment. Report LR-389. Acknowledgement is due to J. C. Basinski, who programed the final equations for the Bendix G-15 computer and did all the numerical work. The author would also like to thank the Director of the National Aeronautical Establishment for permission to publish this paper.

* Senior Research Officer, National Aeronautical Establishment.

1. Introduction

CURRENT interest in orbital gliders and lifting hypersonic vehicles has stimulated both theoretical and experimental work on the prediction of flow fields about such configurations. As a suitable aircraft design developing high lift-drag ratios in hypersonic flight, a flat-top wing-body combination has been proposed in Ref. 1. This configuration consists of a thin, highly swept delta wing beneath which is mounted a half conical body.

Although experimental data on flat-top configurations are being steadily accumulated, there exist relatively few theoretical studies of the flow about such shapes. A method for predicting the aerodynamic forces on flat-top configurations has been presented in Ref. 2. Since it is based on linear theory, its validity is necessarily restricted to the low supersonic speed range. In Ref. 3, a semiempirical method based on the inviscid conical flow equations has been devised for predicting the hypersonic flow about slender flat-top configurations. Although the agreement between the predicted and the experimental surface pressure distribution is remarkably good, the theory is in error because the calculated pressures on the wing do not reduce to those at zero incidence where they are known from the flow about the complete cone.

The purpose of the present investigation is to develop a rational theory of the flow about conical flat-top configurations

traveling at hypersonic speeds and small incidence. Mathematically, the problem involves the solution of the nonlinear conical flow equations in conjunction with a set of boundary conditions, some of which are specified at boundaries (i.e., shock surfaces) whose positions are not known a priori, but must be determined from the solution.

An attractive approach for calculating the supersonic or hypersonic flow about a pointed body is that of the method of linearized characteristics[4] which considers the flow about the body to be a perturbation of a known basic nonlinear flow. Since the flow about a flat-top configuration at small incidence does not depart too much from rotational symmetry, this suggests a perturbation procedure that employs the flow about the circular cone at zero incidence as the basic flow. Only linear terms in the perturbation quantities will be retained in the differential equations and boundary conditions. It should be emphasized that the linearization is with respect to deviations from a known nonlinear flow which is "close" to the actual flow; this is in contrast to the assumption of linearized flow theory where the linearization is with respect to deviation from the uniform flow.

In calculating the supersonic or hypersonic flow about a flat-top configuration, a difficulty arises similar to that in the problem of supersonic flow about complete cones at yaw. Solutions based on perturbations in incidence are not uniformly valid and break down in the vicinity of the cone surface. The nonuniformity is due to the presence of the vortical layer surrounding the cone surface. The flow structure within this layer is complicated, and special mathematical techniques are required for its study.[5, 6] Fortunately, in practical applications where the flow variables are only required at the cone surface, no detailed knowledge of the flow structure within the vortical layer is necessary; only vortical-layer corrections to the flow variables need be applied to give accurate surface values of velocity, temperature, etc.[7] Since there also exists a vortical layer surrounding the body in the present problem, a similar approach will be followed.

2. General Theory

The configuration to be treated is assumed to consist of a half-circular cone mounted beneath a thin delta wing whose leading edge is considered sharp. Under these conditions the wing shock and the cone shock are attached, and the flow fields on the windward and leeward sides of the wing may be treated independently. If the freestream Mach number is assumed large compared to unity, the local pressure coefficient on the expansion side of the wing is approximately equal to zero irrespective of incidence. Since the lifting pressures are then entirely due to the flow on the compression side of the configuration, the theory may also be applied to a wing-body combination whose upper surface is not necessarily flat.

Furthermore, the configuration is assumed to be slender, the body and the wing to have a common apex and to extend to infinity in the streamwise direction. Since there exists no fundamental length, the flow field is independent of distance from the apex and thus conical. If spherical polar coordinates R, θ, ϕ are employed (Fig. 1), the flow is a function of the angular coordinates θ, ϕ only and may be treated in a cross-flow plane.

It is important to pay particular attention to the geometry of the shock waves. The shock system, shown in cross-sectional view in Fig. 2, consists of 1) a plane shock AB attached to the wing leading edge, 2) a cone shock BC, and 3) a curved shock segment BD due to the interaction of the plane and conical shock wave. The existence of the latter may be deduced by appeal to the unsteady flow analogy, according to which the problem becomes equivalent to that of wave interaction in a two-dimensional space. The additional shock segment BD plays the role of the Mach stem in the unsteady analogy, forming a three-shock configuration

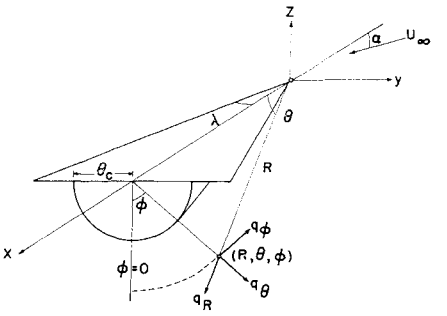

Fig. 1 Schematic diagram of spherical polar coordinate system.

at B and intersecting the wing surface perpendicularly. Since fluid particles undergo different entropy changes according to whether they pass through one shock BC or two shocks AB and BD, a vortex sheet BG must form to allow for the discontinuity in entropy, internal energy, and density. The shock pattern shown in Fig. 2 agrees with that proposed in Ref. 8.

Other qualitative features of the flow may be deduced by extending concepts of the supersonic flow about delta wings at incidence. As shown in Ref. 9, the field on the compression side can be divided into an outboard region where the flow is uniform, two-dimensional (in planes normal to the leading edge), and the equations are of hyperbolic type; and into an inboard region where the flow is nonuniform, three-dimensional, and the equations are of elliptic type. The boundary between the regions is the parabolic surface that is identical with the characteristic conoid emanating from the apex.

If a half-cone is considered mounted beneath the wing, the flow in the outboard and inboard regions is of the same forementioned type, but the boundary between these regions is the shock segment BD (Fig. 2). Since the elliptic region is now bounded by the curved shocks BC and BD, the specific entropy downstream of these shocks must vary from streamline to streamline. This implies that the flow in this region is rotational.

3. Equations of Motion and Boundary Conditions

If one postulates a perfect gas with constant ratio of specific heats γ and constant stagnation enthalpy throughout the medium (since the flow originates in a uniform freestream), the equations appropriate to rotational flow are,[16]

$$\mathbf{q} \times \text{curl } \mathbf{q} = -a^2 \text{ grad } s \tag{1}$$

$$(\mathbf{q}\cdot\nabla)(1/2q^2) = a^2 \text{ div } \mathbf{q} \tag{2}$$

where

$$q^2 = |\mathbf{q}|^2 \tag{3}$$

$$a^2 = \frac{\gamma - 1}{2}(\hat{q}^2 - q^2)$$

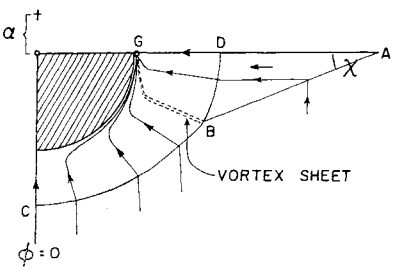

Fig. 2 Shock and streamline pattern at incidence in cross flow plane $x = 1$ [$0 \leq \phi \leq (\pi/2)$].

$$\frac{\hat{q}^2}{U_\infty^2} = 1 + \frac{2}{\gamma - 1}\frac{1}{M_\infty^2} \qquad \text{(Ref. 10)} \qquad (4)$$

is the limit speed and s the nondimensional specific entropy,

$$s = \frac{S - S_\infty}{\gamma(\gamma - 1)c_v} \qquad (5)$$

If Eqs. (1) and (2) are expressed in terms of spherical polar coordinates (R, θ, ϕ, Fig. 1) and all derivatives with respect to R are ignored, the resulting equations describe a conical flow whose velocity components (q_R, q_θ, q_ϕ) satisfy

$$q_\theta \frac{\partial q_R}{\partial \theta} + \frac{q_\phi}{\sin\theta}\frac{\partial q_R}{\partial \phi} - q_\theta^2 - q_\phi^2 = 0 \qquad (6a)$$

$$q_R \frac{\partial q_R}{\partial \theta} - \frac{q_\phi}{\sin\theta}\frac{\partial q_\theta}{\partial \phi} + q_\phi \frac{\partial q_\phi}{\partial \theta} - q_R q_\theta + q_\phi^2 \cot\theta = -\frac{a^2 \partial s}{\partial \theta} \qquad (6b)$$

$$\frac{q_R}{\sin\theta}\frac{\partial q_R}{\partial \phi} + \frac{q_\theta}{\sin\theta}\frac{\partial q_\theta}{\partial \phi} - q_\theta \frac{\partial q_\phi}{\partial \theta} - q_R q_\phi - \cot\theta\, q_\theta q_\phi = -\frac{a^2}{\sin\theta}\frac{\partial s}{\partial \phi} \qquad (6c)$$

$$a^2\left[2q_R + \frac{\partial q_\theta}{\partial \theta} + \frac{1}{\sin\theta}\frac{\partial q_\phi}{\partial \phi} + q_\theta \cot\phi\right] - \left[q_\theta \frac{\partial}{\partial_\theta} + \frac{q_\phi}{\sin\theta}\frac{\partial}{\partial \phi}\right]\left(\frac{q^2}{2}\right) = 0 \qquad (6d)$$

where $q^2 = q_R^2 + q_\theta^2 + q_\phi^2$ and a^2 is given by (3).

The system (6a–6d) must be solved for q_R, q_θ, q_ϕ, and s, subject to the following boundary conditions.

At solid surfaces,

$$q_\theta(\theta_c, \phi) = 0 \qquad |\phi| \le \pi/2$$
$$q_\phi(\theta, \pm\pi/2) = 0 \qquad \theta_c \le \theta \le \lambda \qquad (7)$$

θ_c, λ denoting the semiapex angles of the cone and the wing, respectively.

At shock waves, the boundary conditions immediately downstream of the shocks BC and BD, whose positions are initially unknown, must be found from the well-known jump conditions across shock waves

$$[\rho \mathbf{q}\cdot\mathbf{n}] = 0$$
$$[p + (\rho \mathbf{q}\cdot\mathbf{n})^2] = 0$$
$$\left[\tfrac{1}{2}(\mathbf{q}\cdot\mathbf{n})^2 + \frac{a^2}{\gamma - 1}\right] = 0$$
$$[\mathbf{q} \times \mathbf{n}] = 0$$

where brackets denote the change in the enclosed quantity across the shock, and $\mathbf{n}$ is the unit vector normal to the shock.

If these shock conditions are applied to the shock-segment BC, whose upstream face is in the freestream, the following relations can be shown to hold immediately downstream of the shock BC[11]:

$$q_R/U_\infty = \cos\theta_s \cos\alpha - \sin\alpha \sin\theta_s \cos\phi \qquad (8a)$$

$$q_\theta/U_\infty = -l_b + n_b \cos\delta \sin\delta \qquad (8b)$$

$$q_\phi/U_\infty = l_b \tan\delta + n_b \cos^2\delta \qquad (8c)$$

$$s = \frac{1}{\gamma(\gamma - 1)} \log\left[\frac{p}{p_\infty}\left(\frac{\rho_\infty}{\rho}\right)^\gamma\right] \qquad (8d)$$

where

$$m_b = \cos\alpha \sin\theta_s + \sin\alpha \cos\theta_s \cos\phi + \tan\delta \sin\alpha \sin\phi$$
$$n_b = \sin\alpha \sin\phi - \tan\delta\,(\cos\alpha \sin\theta_s + \sin\alpha \cos\theta_s \cos\phi)$$
$$l_b = \frac{\gamma - 1}{\gamma + 1}\frac{\hat{q}^2}{U_\infty^2}\frac{1}{m_b}\left[1 - \frac{U_\infty^2}{\hat{q}^2}(1 - m_b^2 \cos^2\delta)\right]$$

The equation of the shock segment BC is $\theta = \theta_s(\phi)$, defined within a specific range of ϕ; δ is the angle between the shock normal and a plane ϕ = const, defined by

$$\tan\delta = (1/\sin\theta_s)(d\theta_s/d\phi) \qquad (9)$$

and p/p_∞, ρ/ρ_∞ are the pressure and density ratios across the shock BC given by

$$\frac{p}{p_\infty} = 1 + \frac{\gamma(\gamma - 1)}{\gamma + 1}\frac{\hat{q}^2}{a_\infty^2}\left[\frac{2}{\gamma - 1}\frac{U_\infty^2}{\hat{q}^2} m_b^2 \cos^2\delta + \frac{U_\infty^2}{\hat{q}^2} - 1\right]$$
$$\frac{\rho}{\rho_\infty} = \frac{m_b \cos^2\delta}{l_b}$$

p_∞, ρ_∞, and a_∞ being the pressure, density, and sound velocity of the freestream, respectively.

The boundary conditions that hold immediately downstream of the shock segment BD are calculated similarly. It should be noted, however, that the uniform flow upstream of BD is produced by the shock AB attached to the wing leading edge (Fig. 2). Since the latter is straight and its position known, this uniform flow is readily calculated.[9] Hence, by allowing for these modified upstream conditions, it can be shown that the following relations exist immediately downstream of the shock segment BD[11]:

$$\frac{q_R}{U_\infty} = \left(\cos\alpha \cos^2\lambda + \frac{\bar{M}_2}{M_\infty}\sin\lambda\right)\cos\theta_s + \left(\cos\alpha \sin\lambda - \frac{\bar{M}_2}{M_\infty}\right)\cos\lambda \sin\theta_s |\sin\phi| \qquad (10a)$$

$$q_\theta/U_\infty = -l_w + n_w \cos\delta \sin\delta \qquad (10b)$$

$$q_\phi/U_\infty = l_w \tan\delta + n_w \cos^2\delta \qquad (10c)$$

$$s = s_e + \frac{1}{\gamma(\gamma - 1)} \log\left[\frac{p}{p_e}\left(\frac{\rho_e}{\rho}\right)^\gamma\right] \qquad (10d)$$

where

$$m_w = \left(\cos\alpha \cos^2\lambda + \frac{\bar{M}_2}{M_\infty}\sin\lambda\right)\sin\theta_s + \cos\lambda\left(\cos\alpha \sin\lambda - \frac{\bar{M}_2}{M_\infty}\right) \times (-\cos\theta_s |\sin\phi| + \operatorname{sgn}\phi \tan\delta \cos\phi)$$

$$n_w = \cos\lambda\left(\cos\alpha \sin\lambda - \frac{\bar{M}_2}{M_\infty}\right) \times (\operatorname{sgn}\phi \cos\phi + \tan\delta \cos\theta_s |\sin\phi|) - \left(\cos\alpha \cos^2\lambda + \frac{\bar{M}_2}{M_\infty}\sin\lambda\right)\sin\theta_s \tan\delta$$

$$l_w = \frac{\gamma - 1}{\gamma + 1}\frac{q^2}{U_\infty^2}\frac{1}{m_w}\left[1 - \frac{U_\infty^2}{\hat{q}^2} \times \left(\cos^2\alpha \cos^2\lambda - \frac{\bar{M}_2^2}{M_\infty^2} - m_w^2 \cos^2\delta\right)\right]$$

$$\operatorname{sgn}\phi = \phi/|\phi|$$

The equation of the shock segment BD is $\theta = \theta_s(\phi)$, defined within a specified range of ϕ; δ has the same meaning as in (9). $\bar{M}_2$ is the Mach number of the flow perpendicular to the leading edge downstream of the leading edge shock,

$$\frac{\bar{M}_2}{M_\infty} = (1 - \cos^2\alpha \cos^2\lambda)^{1/2}\frac{\cos\chi'}{\cos\chi}$$

χ is the shock angle shown in Fig. 2 and χ' the angle between the leading edge shock and the component of the freestream velocity perpendicular to the leading edge. χ, χ' are defined by Eqs. (4.2.1) and (4.2.2) of Ref. 9, respectively.

The pressure and density ratio across the shock BD are[11]

$$\frac{p}{p_e} = 1 + \gamma\frac{\gamma-1}{\gamma+1}\frac{\hat{q}^2}{a_e^2}\left[\frac{2}{\gamma-1}\frac{U_\infty^2}{\hat{q}^2}m_w^2\cos^2\delta + \frac{U_\infty^2}{\hat{q}^2}\left(\cos^2\alpha\cos^2\lambda + \frac{\bar{M}_2^2}{M_\infty^2}\right) - 1\right]$$

$$\frac{\rho}{\rho_e} = \frac{m_w^2}{l_w}\cos^2\delta$$

where a_e, p_e, ρ_e, and s_e denote, respectively, the velocity of sound, pressure, density, and specific entropy immediately downstream of the leading edge shock. They are defined by[9]

$$\frac{a_e^2}{a_\infty^2} = 1 + \frac{\gamma-1}{2}\left(1 - \frac{\cos^2\chi'}{\cos^2\chi}\right)(1 - \cos^2\alpha\cos^2\lambda)M_\infty^2$$

$$\frac{p_e}{p_\infty} = 1 + \gamma\sin^2\chi\left(1 - \frac{\tan\chi}{\tan\chi'}\right)(1 - \cos^2\alpha\cos^2\lambda)M_\infty^2$$

$$\frac{\rho_e}{\rho_\infty} = \frac{\tan\chi'}{\tan\chi}$$

$$s_e = \frac{1}{\gamma(\gamma-1)}\log\left[\frac{p_e}{p_\infty}\left(\frac{\rho_\infty}{\rho_e}\right)^\gamma\right]$$

Within the framework of exact inviscid theory, the wing-body problem thus involves the solution to the nonlinear system of Eqs. (6a–6d) for the region bounded by the cone surface, the wing surface, and the shock segments BC, BD. At solid boundaries the boundary conditions are given by (7); at the shocks BC and BD, whose positions $\theta = \theta_s(\phi)$, $R > 0$ are initially unknown, the boundary conditions are given by (8) and (10).

It is evident that the problem as formulated is too complicated to be solved exactly by analytic methods. To render it mathematically tractable, the incidence of the configuration axis will be assumed small compared to the cone semi-apex angle. The flow at small relative incidence can then be treated as a small perturbation of the flow at zero incidence, the latter being presumed known.

4. Flow at Zero Incidence

The characteristics of the flow at zero incidence can be deduced, for instance, from the foregoing discussion by letting $\alpha \to 0$. The principal results are 1) that the shock segments BC and BD merge to form the conical shock $\theta = \theta_{s_0}$, $R > 0$, coaxial with the body cone, where θ_{s_0} is a constant depending on θ_c, M_∞, γ; 2) that the leading edge shock degenerates into a Mach wave whose inclination to the plane of the wing is (Fig. 3)

$$\chi = \sin^{-1}\left(\frac{1}{M_\infty\sin\lambda}\right) \tag{11}$$

and 3) that the parabolic surface is the circular cone

$$\theta = \sin^{-1}\frac{1}{M_\infty} \qquad R > 0$$

For future use it is important to calculate the position of the point of intersection of the Mach wave from the wing leading edge with the cone shock (point B, Fig. 3). If ϕ_B denotes its angular position, it can be shown from the spherical triangle A, B, E (Fig. 3) and by use of (11) that

$$\sin\phi_B = \frac{\cos\theta_{s_0}\cos\lambda \overset{+}{(-)} [(M_\infty^2\sin^2\lambda - 1)(M_\infty^2\sin^2\theta_{s_0} - 1)]^{1/2}}{(M_\infty^2 - 1)\sin\theta_{s_0}\sin\lambda} \tag{12}$$

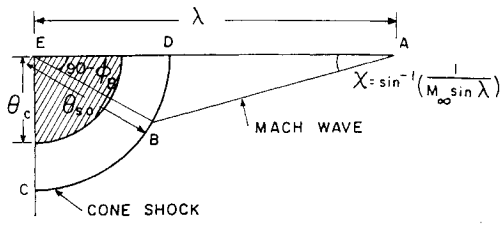

Fig. 3 Cross flow at zero incidence.

Since the parabolic surface must lie either within the shock layer or in a region within the body, this implies that the roots of (12) are real, indicating actual points of intersection; however, only the larger of the roots is of physical interest.

5. Flow at Small Relative Incidence

The flow about the wing-body combination at small relative incidence can now be calculated by means of the perturbation procedure outlined previously. The subsequent development is to some extent similar to that of the flow about the complete cone at small yaw[4, 12]; however, it departs in several important respects because of the different geometry of the configuration and the existence of the shock segments BC and BD.

If quantities associated with the field about the basic cone at zero incidence are denoted by the superscript "0," then $q_R^{(0)}$, $q_\theta^{(0)}$, and $s^{(0)}$ may be regarded as given. Only linear terms in the perturbation quantities will be retained in the differential equations and boundary conditions. To this approximation, series representations of the flow consistent with the differential equations and boundary conditions may be written as

$$\begin{aligned} q_R &= q_R^{(0)} + \frac{\alpha}{\theta_c}\sum_{n=0}^{\infty} u_{2n}\cos 2n\phi \\ q_\theta &= q_\theta^{(0)} + \frac{\alpha}{\theta_c}\sum_{n=0}^{\infty} v_{2n}\cos 2n\phi \\ q_\phi &= \frac{\alpha}{\theta_c}\sum_{n=0}^{\infty} w_{2n}\sin 2n\phi \\ s &= s^{(0)} + \frac{\alpha}{\theta_c}\sum_{n=0}^{\infty} s_{2n}\cos 2n\phi \end{aligned} \tag{13}$$

where u_{2n}, v_{2n}, and w_{2n} are functions of θ to be determined, $w_0 = 0$ for convenience, and the s_{2n} are unknown constants.

Similarly, the shock wave angle θ_s is expanded in a Fourier series

$$\theta_s(\phi) = \theta_{s_0} + \frac{\alpha}{\theta_c}\sum_{n=0}^{\infty} b_{2n}\cos 2n\phi \tag{14}$$

where θ_{s0} is the shock wave angle for the basic cone and the b_{2n} are constants to be determined.

When the series (13) are substituted into the system (6a–6d), and coefficients of like powers in α/θ_c are equated, an infinite set of differential equations results. As expected, $q_R^{(0)}$, $q_\theta^{(0)}$, and $s^{(0)}$ satisfy the differential equations for axially symmetrical conical flow

$$\left.\begin{aligned} \frac{dq_R^{(0)}}{d\theta} - q_\theta^{(0)} &= 0 \\ a_0^2\left[2q_R^{(0)} + \frac{dq_\theta^{(0)}}{d\theta} + q_\theta^{(0)}\cot\theta\right] &= q_\theta^{(0)}\frac{d}{d\theta}\left(\frac{q_0^2}{2}\right) \\ \frac{ds^{(0)}}{d\theta} &= 0 \end{aligned}\right\} \tag{15}$$

where

$$a_0^2 = \frac{\gamma - 1}{2}\left[\hat{q}^2 - q_R^{(0)2} - q_\theta^{(0)2}\right] \qquad q_0^2 = q_R^{(0)2} + q_\theta^{(0)2} \tag{16}$$

whereas the Fourier coefficients of the perturbed field satisfy the series of ordinary differential equations.

$n = 0$:

$$(a_0^2 - q_\theta^{(0)2})u_0'' + \left\{a_0^2 \cot\theta - \left[(\gamma - 1)\frac{q_\theta^{(0)2}}{a_0^2} + 1\right] \times \frac{d}{d\theta}\left(\frac{q_0^2}{2}\right) - q_\theta^{(0)}\left(\frac{dq_\theta^{(0)}}{d\theta} + q_R^{(0)}\right)\right\} u_0' + \left[2a_0^2 - (\gamma - 1)\frac{q_R^{(0)}q_\theta^{(0)}}{a_0^2}\frac{d}{d\theta}\left(\frac{q_0^2}{2}\right) - q_\theta^{(0)2}\right] u_0 = 0 \tag{17a}$$

$$v_0 = u_0'$$

$n \geq 1$:

$$-\frac{q_\theta^{(0)}}{\sin\theta} 2nu_{2n}' - \frac{q_R^{(0)}}{\sin\theta} 2nu_{2n} - q_\theta^{(0)}w_{2n}' - (q_R^{(0)} + q_\theta^{(0)}\cot\theta)w_{2n} = \frac{a_0^2}{\sin\theta} 2ns_{2n}$$

$$(a_0^2 - q_\theta^{(0)2})u_{2n}'' + \left[a_0^2 \cot\theta - \left((\gamma - 1)\frac{q_\theta^{(0)2}}{a_0^2} + 1\right) \times \frac{d}{d\theta}\left(\frac{q_0^2}{2}\right) - q_\theta^{(0)}\left(\frac{dq_\theta^{(0)}}{d\theta} + q_R^{(0)}\right)\right] u_{2n}' + \left[2a_0^2 - (\gamma - 1)\frac{q_R^{(0)}q_\theta^{(0)}}{a_0^2}\frac{d}{d\theta}\left(\frac{q_0^2}{2}\right) - q_\theta^{(0)2}\right] u_{2n} + \frac{a_0^2}{\sin\theta} 2nw_{2n} = 0 \tag{17b}$$

$$v_n = u_n'$$

primes denoting differentiation with respect to θ.

The system (17b) is identical with that associated with the supersonic flow about cones at small yaw[12] except that s_{2n} is now defined differently. It possesses the first integral

$$2nu_{2n} + \sin\theta w_{2n} = -2n \sin\theta T_{2n}(\theta) \tag{18}$$

where

$$T_{2n}(\theta) = s_{2n}(-q_\theta^{(0)})^{1/2}(\sin\theta)^{-1/2}a_0^{1/(\gamma-1)} \times \int_{\theta_{s_0}}^{\theta} \frac{a_0^{(2\gamma-3)/(\gamma-1)}d\theta}{(-q_\theta^{(0)})^{3/2}(\sin\theta)^{1/2}} \qquad n \geq 0 \tag{19}$$

It should be noted that the foregoing formulation applies to configurations of arbitrary cone angle and arbitrary leading edge sweep, flying at supersonic or hypersonic speeds and small relative incidence. Because terms of order α^2/θ_c^2 have been omitted in this formulation, first-order quantities will differ from their exact values by $0(\alpha^2/\theta_c^2)$.

It seems unlikely that the foregoing differential equations admit analytic solutions. Hence they may have to be solved numerically.

6. Hypersonic Approximations

The theory is rendered more tractable by introducing the hypersonic small-disturbance approximation. To this end, it is assumed that

$$M_\infty \to \infty,\ \theta_c \to 0 \text{ such that } M_\infty\theta_c \sim 1 \text{ or } \gg 1,\ \lambda \sim \theta_c \tag{20}$$

In addition, it is assumed that the shock wave is "close" to the body, i.e.,

$$[(\theta - \theta_c)/\theta_c] \ll 1 \tag{21a}$$

which implies that

$$\cos\theta \approx 1,\ \cot\theta \approx \frac{1}{\sin\theta} \approx \frac{1}{\theta} \text{ for } \theta_c \leq \theta \leq \theta_{s_0} \tag{21b}$$

Eq. (21a) implies the assumptions

$$\gamma - 1 \ll 1 \qquad \frac{1}{M_\infty^2\theta_c^2} \ll 1$$

as may be shown by means of the formula for θ_{s_0} [cf. (27)].

If these assumptions are introduced and squares and higher powers of small quantities are discarded, a first-order hypersonic theory can be developed which can be expected to provide a close approximation for slender configurations at small incidence.

If w_{2n} and w_{2n}' are eliminated between (17b) and (18) and the approximations (20, 21a, 21b) are introduced, (17a) and (17b) simplify to

$$\theta^2u_0'' + \theta u_0' + 2\theta^2u_0 = 0 \qquad n = 0 \tag{22a}$$

$$\theta^2u_{2n}'' + \theta u_{2n}' - 4n^2u_{2n} = 4n^2T_{2n}(\theta) \qquad n \geq 1 \tag{22b}$$

where T_{2n} is to be understood as the hypersonic approximation to (19), namely,

$$T_{2n}(\theta) = s_{2n}\frac{\gamma - 1}{2}\frac{\hat{q}^2 - U_\infty^2}{U_\infty\theta_c} \times \left[1 - \left(\frac{\theta_{s_0}}{\theta}\right)^{1/2}\left(\frac{\theta - \theta_c}{\theta_{s_0} - \theta_c}\right)^{1/2}\right] \qquad n \geq 0 \tag{23}$$

Substituting (13) into (8) and (10), expanding $q_R^{(0)}$, $q_\theta^{(0)}$, u_{2n}, v_{2n}, and w_{2n} in Taylor series around $\theta = \theta_{s_0}$, the boundary conditions (8) and (10) can be made to yield the following relations for u_{2n}, v_{2n}, etc., at $\theta = \theta_{s_0}$, valid for $n \geq 0$:

$$\frac{u_{2n}(\theta_{s_0})}{U_\infty} = -b_{2n}(1 - \epsilon)\theta_{s_0} + g_{2n}(\theta_{s_0}) \tag{24a}$$

$$\frac{u_{2n}'(\theta_{s_0})}{U_\infty} = \frac{v_{2n}(\theta_{s_0})}{U_\infty} = \frac{2}{\gamma + 1}b_{2n}(2 + \epsilon) + k_{2n}(\theta_{s_0}) \tag{24b}$$

$$\frac{w_{2n}(\theta_{s_0})}{U_\infty} = (1 - \epsilon)2nb_{2n} + h_{2n}(\theta_{s_0}) \tag{24c}$$

$$s_{2n} = \left[\frac{ds^{(0)}}{d\theta}\right]_{\theta=\theta_{s_0}} b_{2n} + j_{2n}(\theta_{s_0}) \tag{24d}$$

where

$$\epsilon = \frac{\gamma - 1}{\gamma + 1} + \frac{2}{\gamma + 1}\frac{1}{M_\infty^2\theta_{s_0}^2} \tag{25}$$

$$\left[\frac{ds^{(0)}}{d\theta}\right]_{\theta=\theta_{s_0}} = \frac{1}{\theta_{s_0}} \times \frac{(M_\infty^2\theta_{s_0}^2 - 1)^2}{\{\gamma M_\infty^2\theta_{s_0}^2 - [(\gamma - 1)/2]\}\{1 + [(\gamma - 1)/2]M_\infty^2\theta_{s_0}^2\}} \tag{26}$$

are the density ratio across the bow shock when $\alpha = 0$ and the rate of change of entropy with respect to shock angle, respectively.[4] θ_{s_0} is defined by

$$\frac{\theta_{s_0}}{\theta_c} = \frac{\gamma + 1}{\gamma + 3} + \left[\left(\frac{\gamma + 1}{\gamma + 3}\right)^2 + \frac{2}{\gamma + 3}\frac{1}{M_\infty^2\theta_c^2}\right]^{1/2} \tag{Ref. 13) (27}$$

whereas the g_{2n}, h_{2n}, j_{2n}, and k_{2n} are obtained by application of Fourier analysis to the right-hand sides of the linearized forms of boundary conditions (8) and (10). To demonstrate the procedure, g_{2n} will be calculated explicitly. To this end the right-hand sides of (8a) and (10a) are combined by defining a function $G(\theta, \phi, \alpha)$, say, which may be approximated by

$$G(\theta, \phi, \alpha) = G^{(0)}(\theta) + (\alpha/\theta_c)\, G^{(1)}(\theta, \phi)$$

where

$$G^{(0)}(\theta) = \cos\theta$$

corresponds to the axially-symmetrical flow, and

$$G^{(1)}(\theta, \phi) = \begin{cases} -\sin\theta\cos\phi & |\phi| < \phi_B \\ \dfrac{-\sin\lambda\cos\theta + \cos\lambda\sin\theta|\sin\phi|}{(M_\infty^2\sin^2\lambda - 1)^{1/2}} & \phi_B < |\phi| \leq \pi/2 \end{cases}$$

Defining $G^{(1)}(\theta, \phi)$ outside the interval $|\phi| \leq \pi/2$ by its periodic extension, putting

$$G^{(1)}(\theta, \phi) = \sum_{n=0}^{\infty} g_{2n}(\theta)\cos 2n\phi$$

and introducing the hypersonic approximations (20), (21) yields

$$\left.\begin{aligned} g_0(\theta) &= \frac{2}{\pi}\int_0^{\pi/2} G^{(1)}(\theta, \phi)d\phi = \\ &\quad -\frac{2\theta}{\pi}\left[\sin\phi_B + \frac{(\lambda/\theta)[(\pi/2) - \phi_B] - \cos\phi_B}{(M_\infty^2\lambda^2 - 1)^{1/2}}\right] \\ g_{2n}(\theta) &= \frac{4}{\pi}\int_0^{\pi/2} G^{(1)}(\theta, \phi)\cos 2n\phi d\phi = \\ &\quad -\frac{2\theta}{\pi}\left\{\frac{\sin(2n+1)\phi_B}{2n+1} + \frac{\sin(2n-1)\phi_B}{2n-1} - \right. \\ &\quad \frac{1}{(M_\infty^2\lambda^2 - 1)^{1/2}}\left[\frac{\lambda}{\theta}\frac{\sin 2n\phi_B}{2n} + \frac{\cos(2n+1)\phi_B}{2n+1} - \right. \\ &\quad \left.\left.\left.\frac{\cos(2n-1)\phi_B}{2n-1}\right]\right\} \qquad n \geq 1 \end{aligned}\right\} \quad (28a)$$

Proceeding similarly with the boundary conditions (8b), (10b) etc., explicit expressions for h_{2n}, j_{2n}, and k_{2n} are derived. These are

$$\left.\begin{aligned} h_0 &= 0 \\ h_{2n} &= \frac{2}{\pi}\left\{\frac{\sin(2n-1)\phi_B}{2n-1} - \frac{\sin(2n+1)\phi_B}{2n+1} + \right. \\ &\quad \frac{1}{(M_\infty^2\lambda^2 - 1)^{1/2}}\left[\frac{\cos(2n+1)\phi_B}{2n+1} + \right. \\ &\quad \left.\left.\frac{\cos(2n-1)\phi_B}{2n-1}\right]\right\} \qquad n \geq 1 \end{aligned}\right\} \quad (28b)$$

$$\left.\begin{aligned} j_0(\theta) &= \frac{2}{\pi}\frac{1}{\theta}\left[\frac{ds^{(0)}}{d\theta}\right]\left\{\sin\phi_B - \frac{1}{(M_\infty^2\lambda^2 - 1)^{1/2}} \times \right. \\ &\quad \left.\left[\frac{\gamma - 1}{2}\frac{\lambda}{\theta}M_\infty^2\theta^2\left(\frac{\pi}{2} - \phi_B\right) + \cos\phi_B\right]\right\} \\ j_{2n}(\theta) &= \frac{2}{\pi}\frac{1}{\theta}\left[\frac{ds^{(0)}}{d\theta}\right]\left\{\frac{\sin(2n+1)\phi_B}{2n+1} + \right. \\ &\quad \frac{\sin(2n-1)\phi_B}{2n-1} + \frac{1}{(M_\infty^2\lambda^2 - 1)^{1/2}} \times \\ &\quad \left[(\gamma - 1)\frac{\lambda}{\theta}M_\infty^2\theta^2\frac{\sin 2n\phi_B}{2n} + \frac{\cos(2n-1)\phi_B}{2n-1} - \right. \\ &\quad \left.\left.\left.\frac{\cos(2n+1)\phi_B}{2n+1}\right]\right\} \qquad n \geq 1 \end{aligned}\right\} \quad (28c)$$

$$k_0(\theta) = -\frac{2}{\pi}\left\{\left(2\frac{\gamma - 1}{\gamma + 1} - \epsilon\right)\sin\phi_B + \frac{1}{(M_\infty^2\lambda^2 - 1)^{1/2}}\left[2\frac{\lambda}{\theta}\frac{\gamma - 1}{\gamma + 1}\left(\frac{\pi}{2} - \phi_B\right) - \left(2\frac{\gamma - 1}{\gamma + 1} - \epsilon\right)\cos\phi_B\right]\right\}$$

[*The second part of Eq. (28d) is in the following column.*]

$$k_{2n}(\theta) = -\frac{2}{\pi}\left\{\left(2\frac{\gamma - 1}{\gamma + 1} - \epsilon\right) \times \left(\frac{\sin(2n+1)\phi_B}{2n+1} + \frac{\sin(2n-1)\phi_B}{2n-1}\right) - \frac{1}{(M_\infty^2\lambda^2 - 1)^{1/2}} \times \left[4\frac{\lambda}{\theta}\frac{\gamma - 1}{\gamma + 1}\frac{\sin 2n\phi_B}{2n} + \left(2\frac{\gamma - 1}{\gamma + 1} - \epsilon\right)\left(\frac{\cos(2n+1)\phi_B}{2n+1} - \frac{\cos(2n-1)\phi_B}{2n-1}\right)\right]\right\} \qquad n \geq 1 \quad (28d)$$

where ϵ and $[ds^{(0)}/d\theta]$ are given by (25) and (26), respectively.

7. Explicit Solutions for the Flow Field

The solution to the series of differential equations (22a) and (22b), satisfying the boundary conditions (24a–24d) and $u_{2n}'(\theta_c) = 0$ [cf. (7)], can now be found for each value of n separately. It can be shown that the boundary conditions are sufficient to determine b_{2n}, $u_{2n}(\theta)$, and $v_{2n}(\theta)$ uniquely for each n. For $n = 0$ these are approximately

$$b_0 = -\frac{\gamma + 1}{2(\epsilon + 2)}k_0(\theta_{s_0}) \quad (29a)$$

$$\left.\begin{aligned} \frac{u_0(\theta)}{U_\infty} &= [g_0(\theta_{s_0}) - b_0(1 - \epsilon)\theta_{s_0}][1 + 0(\theta_c^2)] \\ \frac{v_0(\theta)}{U_\infty} &= -[g_0(\theta_{s_0}) - b_0(1 - \epsilon)\theta_{s_0}]\left(\frac{\theta}{\theta_c} - \frac{\theta_c}{\theta}\right)\theta_c \end{aligned}\right\} \quad (29b)$$

whereas, for $n \geq 1$,

$$\begin{aligned} b_{2n} &= \left\{\frac{2n}{M_\infty^2\theta_{s_0}^2}\left(1 + \frac{\gamma - 1}{2}M_\infty^2\theta_{s_0}^2\right)\theta_{s_0}j_{2n}\frac{I_{2n}}{\theta_c} + \right. \\ &\quad \frac{g_{2n}}{\theta_{s_0}}\left[\left(\frac{\theta_{s_0}}{\theta_c}\right)^{2n} - \left(\frac{\theta_c}{\theta_0}\right)^{2n}\right] - \frac{k_{2n}}{2n}\left[\left(\frac{\theta_{s_0}}{\theta_c}\right)^{2n} + \left(\frac{\theta_c}{\theta_{s_0}}\right)^{2n}\right]\Bigg\} \times \\ &\quad \left\{\frac{2n}{M_\infty^2\theta_{s_0}^2}\frac{(M_\infty^2\theta_{s_0}^2 - 1)^2}{[(\gamma - 1)/2] - \gamma M_\infty^2\theta_{s_0}^2}\frac{I_{2n}}{\theta_c} + \frac{2}{\gamma + 1} \times \right. \\ &\quad \left(1 - \frac{1}{M_\infty^2\theta_{s_0}^2}\right)\left[\left(\frac{\theta_{s_0}}{\theta_c}\right)^{2n} - \left(\frac{\theta_c}{\theta_{s_0}}\right)^{2n}\right] + \frac{1}{n}\frac{1}{(\gamma + 1)^2} \times \\ &\quad \left.\left.\left(3\gamma + 1 + \frac{2}{M_\infty^2\theta_{s_0}^2}\right)\left[\left(\frac{\theta_{s_0}}{\theta_c}\right)^{2n} + \left(\frac{\theta_c}{\theta_{s_0}}\right)^{2n}\right]\right\}^{-1} \end{aligned} \quad (29c)$$

where

$$I_{2n} = \int_{\theta_c}^{\theta_{s_0}}\left[1 - \left(\frac{\theta_{s_0}}{t}\right)^{1/2}\left(\frac{t - \theta_c}{\theta_{s_0} - \theta_c}\right)^{1/2}\right] \times \left[\left(\frac{\theta_c}{t}\right)^{2n} + \left(\frac{t}{\theta_c}\right)^{2n}\right]dt$$

$$\begin{aligned} \frac{u_{2n}(\theta)}{\theta_c U_\infty} &= -\frac{n\theta_{s_0}}{\theta_c}\frac{\theta}{\theta_c}\left[\frac{b_{2n}}{M_\infty^2\theta_{s_0}^2}\frac{(M_\infty^2\theta_{s_0}^2 - 1)^2}{\gamma M_\infty^2\theta_{s_0}^2 - [(\gamma - 1)/2]} + \right. \\ &\quad \left.\theta_{s_0}j_{2n}\left(\frac{\gamma - 1}{2} + \frac{1}{M_\infty^2\theta_{s_0}^2}\right)\right] \times \\ &\quad \left\{\frac{1}{2n+1}\left[1 - \frac{y}{y_s} - \left(\frac{\theta_c}{\theta}\right)^{2n+1}\left(1 - \frac{J_{2n+1}(y)}{y_s}\right)\right] + \right. \\ &\quad \frac{1}{2n-1}\left[1 - \frac{y}{y_s} + \left(\frac{\theta_c}{\theta}\right)^{2n+1}\left(1 - \frac{K_{2n+1}(y_s)}{y_s}\right) - \right. \\ &\quad \left.\left.\frac{\hat{I}_{2n-1}(\theta)}{y_s}\right]\right\} + \frac{1}{2}\left[\frac{u_{2n}(\theta_{s_0})}{\theta_c U_\infty} + \frac{\theta_{s_0}/\theta_c}{2n}\frac{v_{2n}(\theta_{s_0})}{U_\infty}\right] \times \\ &\quad \left(\frac{\theta}{\theta_{s_0}}\right)^{2n}\left[1 + \left(\frac{\theta_c}{\theta}\right)^{4n}\right] \end{aligned} \quad (29d)$$

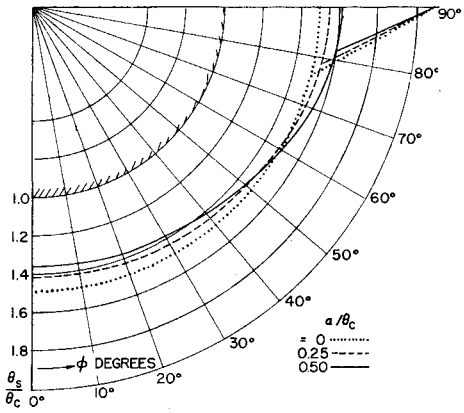

Fig. 4 Shock shape for family of configurations with $\lambda/\theta_c = 2.09$ and $M_\infty\theta_c = 1$.

where, for brevity,

$$y = \left(1 - \frac{\theta_c}{\theta}\right)^{1/2} \qquad y_s = \left(1 - \frac{\theta_c}{\theta_{s_0}}\right)^{1/2} \tag{30}$$

$$J_{2n+1}(y) = \int_0^y \frac{dx}{(1 - x^2)^{2n+1}} \tag{31a}$$

$$K_{2n+1}(y) = \int_0^y (1 - x^2)^{2n+1} dx$$

The J_{2n+1}, K_{2n+1} can be shown to satisfy the recursion relations:

$$J_{2n+1}(y) = \frac{(4n-1)(4n-3)}{4n(4n-2)} J_{2n-1}(y) + \frac{1}{8n}\frac{y}{(1-y^2)^{2n-1}}\left[\frac{4n-1}{2n-1} + \frac{2}{1-y^2}\right] \qquad n \geq 1 \tag{31b}$$

$$J_1(y) = \tanh^{-1} y = \frac{1}{2}\log\frac{1+y}{1-y}$$

$$\left.\begin{aligned} K_{2n+1}(y) &= \frac{(4n+2)4n}{(4n+3)(4n+1)} K_{2n-1}(y) + \frac{y(1-y^2)^{2n+1}}{4n+3}\left[1 + \frac{4n+2}{4n+1}\frac{1}{1-y^2}\right] \qquad n \geq 1 \\ K_1(y) &= y[1 - (y^2/3)] \\ \hat{I}_{2n-1}(\theta) &= \left(\frac{\theta}{\theta_c}\right)^{2n-1}[K_{2n-1}(y_s) - K_{2n-1}(y)] \end{aligned}\right\} \tag{31c}$$

Since the sequences of functions $J_{2n+1}(y)$, $K_{2n+1}(y)$, $n = 0, 1, 2$ depend only on elementary functions of y (algebraic and logarithmic), it follows from (29b, 29d, and 30) that each $u_{2n}(\theta)$ for $n \geq 0$ consists only of elementary functions of θ/θ_c.

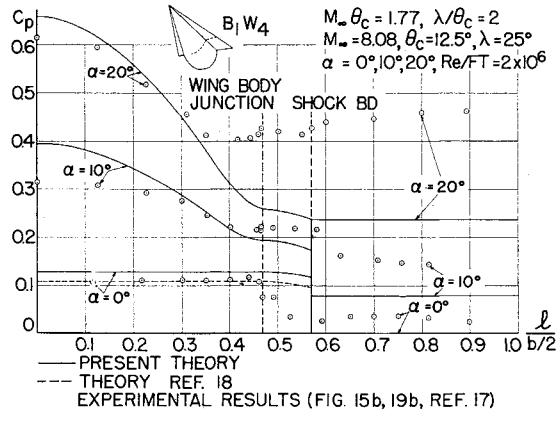

Fig. 5 Spanwise pressure distribution on lower surface of model B_1W_4.[17]

The Fourier coefficients of other flow variables are readily calculated. For $n = 0$, they are given by (29a) and (29b), whereas, for $n \geq 1$, v_{2n} follows by differentiation of (29d) with respect to θ [cf. (17b)]; s_{2n} from (24d); and w_{2n} from (18, 19, and 29d). Whence the velocity and entropy fields external to the vortical layer are completely defined by (13) and the shape of the bow shock by (14, 29a, and 29c).

8. Surface Pressures and Aerodynamic Forces

If flow properties are to be evaluated at the cone surface, the presence of the vortical layer surrounding the body must be taken into account. The calculation procedure is similar to that of the flow about complete cones at small yaw.[7] The only difference is in the position of the vortical singularity where the velocity is many-valued, the vorticity is infinite but the pressure is single-valued. Since, for small incidence, the vortical singularity coincides with the stagnation point of the cross flow where $q_\theta = q_\phi = 0$,[14] it follows that, in the case of a flat-top configuration, the vortical singularity must lie in the wing-body junction. By applying arguments similar to the case of cones at yaw,[4] it can be shown that the entropy on the cone surface must be equal to the constant value that exists in the meridian plane $\phi = 0$. On the other hand, the entropy field external to the vortical layer as given by (13) is the system of planes $\phi = \text{const}$ which appear as a pencil of lines in the cross-flow plane (Fig. 2).

To calculate the spanwise pressure distribution on the configuration surface, use can be made of known results for cones at yaw[7]; namely that, to the present order of accuracy, the pressure is simply transmitted across the vortical layer, i.e., the approximate pressure field external to the vortical layer is uniformly valid right to the cone surface. It can be calculated by means of the thermodynamic relation

$$\frac{p}{p_\infty} = \left(\frac{a^2}{a_\infty^2}\right)^{\gamma/(\gamma-1)} e^{-\gamma s} \tag{32}$$

where a^2 and s are given by (3) and (13), respectively. If these are substituted into (32), and relevant hypersonic approximations are introduced, the pressure distribution on the surface of the configuration can be expressed as follows:

On the cone surface,

$$\frac{C_p(\theta_c, \phi)}{\theta_c^2} = \frac{C_p^{(0)}(\theta_c)}{\theta_c^2} - \frac{2\alpha}{\theta_c}\frac{\rho^{(0)}(\theta_c)}{\rho_\infty}\sum_{n=0}^{\infty}\frac{u_{2n}(\theta_c)}{\theta_c U_\infty}\cos 2n\phi \qquad |\phi| \leq \frac{\pi}{2} \tag{33}$$

where

$$\frac{C_p^{(0)}(\theta_c)}{\theta_c^2} = \frac{4}{\gamma+1}\frac{\theta_{s_0}^2}{\theta_c^2}\left(1 - \frac{1}{M_\infty^2\theta_{s_0}^2}\right) \qquad \text{(Ref. 13)} \tag{34}$$

is the pressure coefficient at zero incidence and

$$\frac{\rho^{(0)}(\theta)}{\rho_\infty} = \frac{1}{\epsilon} \qquad \text{[cf. (25)]}$$

the corresponding density field.

On the compression side of the wing, between the junction and the shock BD.

$$\frac{C_p}{\theta_c^2}\left(\theta, \frac{\pi}{2}\right) = \frac{C_p^{(0)}(\theta)}{\theta_c^2} - \frac{2\rho^{(0)}(\theta)}{\rho_\infty}\frac{\alpha}{\theta_c}\sum_{n=0}^{\infty}(-1)^n \times \left[\frac{q_R^{(0)}(\theta)u_{2n}(\theta)}{\theta_c U_\infty^2} + \frac{q_\theta^{(0)}(\theta)v_{2n}(\theta)}{\theta_c U_\infty^2}\right] \qquad \theta_c \leq \theta \leq \theta_{s_0} \tag{35}$$

where $\rho^{(0)}(\theta)/\rho_\infty$ and $C_p^{(0)}(\theta)/\theta_c^2$ are approximately given by (25) and (34), respectively.

Between the shock BD and the wing leading edge,

$$\frac{C_p}{\theta_c^2}\left(\theta, \frac{\pi}{2}\right) = \frac{2(\alpha\lambda/\theta_c^2)}{(M_\infty^2\lambda^2 - 1)^{1/2}} \qquad \theta_{s_0} \leq \theta \leq \lambda \quad (36)$$

i.e., the pressure is uniform.

Since both the entropy and the pressure distribution on the cone surface are thereby known, any other thermodynamic variable can be evaluated using the perfect gas equation of state relating that variable and the pressure and the entropy. For instance, the density and temperature distribution on the cone surface are

$$\frac{\rho(\theta_c, \phi)}{\rho_\infty} = \frac{1}{\epsilon}\left[1 - \frac{\alpha}{\theta_c}\frac{a_\infty^2}{a_0^2} M_\infty^2\theta_c^2 \sum_{n=0}^{\infty} \frac{u_{2n}(\theta_c)}{\theta_c U_\infty} \cos 2n\phi\right] \qquad |\phi| \leq \frac{\pi}{2}$$

$$\frac{T(\theta_c, \phi)}{T_\infty} = \left[\frac{a(\theta_c, \phi)}{a_\infty}\right]^2 = \frac{a_0^2}{a_\infty^2}\left[1 - (\gamma - 1)\frac{\alpha}{\theta_c}\frac{a_\infty^2}{a_0^2} M_\infty^2\theta_c^2 \sum_{n=0}^{\infty} \frac{u_{2n}(\theta_c)}{\theta_c U_\infty} \cos 2n\phi\right] \qquad |\phi| \leq \frac{\pi}{2}$$

where a_0 is the sound velocity at the cone surface at zero incidence, defined by (16). Surface values of velocity components may be obtained as in Ref. 7.

By integrating the surface pressures about the exposed area of the body and the windward side of the wing, the normal and axial force and, hence, the lift and drag, can be calculated. It will suffice to quote relevant formulas from Ref. 11:

$$\frac{C_{N_b}}{\theta_c^2} = \frac{\theta_c}{\lambda}\left[\frac{C_p^{(0)}(\theta_c)}{\theta_c^2} + \frac{2\alpha}{\theta_c}\frac{\rho^{(0)}(\theta)}{\rho_\infty} \sum_{n=0}^{\infty} \frac{(-1)^n}{(2n+1)(2n-1)} \frac{u_{2n}(\theta_c)}{\theta_c U_\infty}\right]$$

$$\frac{C_{N_w}}{\theta_c^2} = \frac{4}{\gamma + 1}\left(1 - \frac{1}{M_\infty^2\theta_{s_0}^2}\right)\left(\frac{\theta_{s_0}}{\theta_c} - 1\right)\frac{\theta_{s_0}^2}{\lambda\theta_c} - \frac{2\alpha}{\theta_c}\sum_{n=0}^{\infty}(-1)^n\Omega_{2n} + \frac{(2\alpha/\theta_c)[(\lambda/\theta_c) - (\theta_{s_0}/\theta_c)]}{(M_\infty^2\lambda^2 - 1)^{1/2}}$$

$$\frac{C_{A_b}}{\theta_c^3} = \frac{\pi}{2}\frac{\theta_c}{\lambda}\left[\frac{C_p^{(0)}(\theta_c)}{\theta_c^2} - \frac{2\alpha}{\theta_c}\frac{\rho^{(0)}(\theta_c)}{\rho_\infty}\frac{q_R^{(0)}(\theta_c)}{U_\infty}\frac{u_0(\theta_c)}{\theta_c U_\infty}\right]$$

$C_{A_w} = 0$ (since the leading edge is assumed sharp)

where

$$\Omega_{2n} = \int_{\theta_c}^{\theta_{s_0}} \frac{\rho^{(0)}(\theta)}{\rho_\infty}\left[\frac{q_R^{(0)}(\theta)}{U_\infty}\frac{u_{2n}(\theta)}{\theta_c U_\infty} + \frac{q_\theta^{(0)}(\theta)}{\theta_c U_\infty}\frac{u_{2n}'(\theta)}{U_\infty}\right] d\theta$$

whence the lift and pressure drag coefficients become

$$\frac{C_L}{\theta_c^2} = \frac{C_{N_b}}{\theta_c^2} + \frac{C_{N_w}}{\theta_c^2}$$

$$\frac{C_D}{\theta_c^3} = \frac{C_{A_b}}{\theta_c^3} + \frac{\alpha}{\theta_c}\frac{C_L}{\theta_c^2}$$

The effect of both base-pressure drag and skin-friction drag are here ignored.

It should be noted that all formulas deduced clearly show the dependence on the various hypersonic similarity parameters[15]; thus they apply to a family of configurations.

9. Numerical Results

To check the theoretical analysis, numerical calculations were carried out on a Bendix G-15 digital computer. The quantities computed include the shock shape, the surface pressure distribution, and the aerodynamic forces.

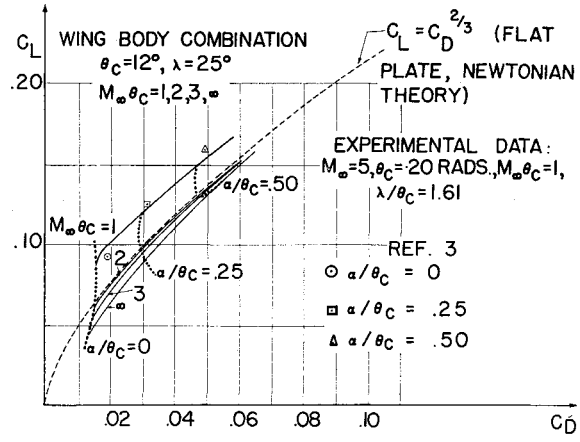

Fig. 6 Drag polars.

The results of these calculations for the shape of the bow shock for a family of configurations with $\lambda/\theta_c = 2.09$, $M_\infty\theta_c = 1$, and $\alpha/\theta_c = 0$, 0.25 and 0.50 are displayed in Fig. 4. It is evident that, as α/θ_c increases, the shock shape departs more and more from that of a circular cone.

The predicted spanwise pressure distribution on a configuration with $\theta_c = 12.5°$, $\lambda = 25°$ at incidences of 0°, 10°, and 20° in a Mach 8 flow is compared with corresponding experimental results[17] in Fig. 5 (l measures the spanwise distance from the windward generator, and b is the total wing span). It is seen that theoretical and experimental pressure distributions on the body agree reasonably (even at high relative incidence) but that significant departures occur near the corner and out on the wing. These are believed mainly to be due to the interaction of the shock BD with the wing boundary layer causing flow separation. Although the theory holds strictly only for $\alpha \ll \theta_c \ll 1$, the departures between theory and experiment appear to be independent of α/θ_c; this indicates that the theory may also be valid when $\alpha \sim \theta_c$.

Predicted drag polars for the same configuration at $\alpha/\theta_c = 0$, 0.25, 0.50 and $M_\infty\theta_c = 1$, 2, 3, ∞ are shown together with the drag polar for a two-dimensional flat plate (calculated by Newtonian theory) in Fig. 6. It is seen that the latter is an asymptote of the family of polars and that the approach to it becomes more rapid with increase of both α/θ_c and $M_\infty\theta_c$. This is consistent with physical reasoning since at large incidence the flow about the configuration resembles more closely that about the wing alone. For the purpose of comparison, experimental drag polars corresponding to $M_\infty\theta_c = 1$, available from Ref. 3, are included in this figure.

The variation of lift-drag ratio with lift coefficient for the foregoing configuration at $M_\infty\theta_c = 1$, 2, 3 and ∞ at $\alpha/\theta_c = 0$, 0.25, and 0.50 is illustrated in Fig. 7. It is seen that the maximum lift-drag ratio occurs at $\alpha/\theta_c = 0$ and that this maximum is approximately 5 for the configuration under consideration ($M_\infty = 5$).

10. Conclusions

By combining the hypersonic small disturbance approximation with the theory of linearized characteristics, explicit expressions for the bow shock wave and the perturbation velocity field are obtained for conical flat-top configurations traveling at hypersonic speed and small incidence. Once the perturbation velocities are determined, the surface pressure distribution and over-all aerodynamic forces are readily calculated.

The most significant feature of the theory is that it provides an analytic solution to the problem, based upon rigorous

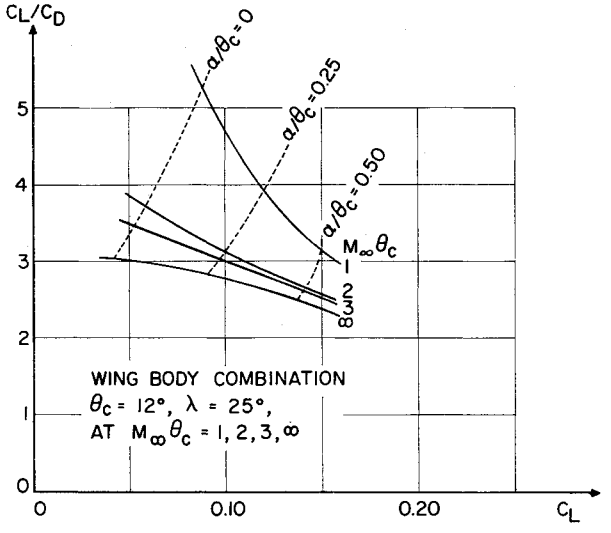

Fig. 7 Lift-drag ratio.

formal procedures. In applying the theory to an actual case, no restriction need be imposed on the magnitude of the cone angle or the leading edge sweep, except the usual smallness criteria for hypersonic small-disturbance theory. Although formally the theory is strictly applicable only for $\alpha \ll \theta_c \ll 1$, it is likely to be also valid for $\alpha/\theta_c \sim 1$, as is usually the case for small perturbation theories.[19] The accuracy of the theory is mainly controlled by the similarity parameter $M_\infty\theta_c$ and improves as $M_\infty\theta_c \to \infty$.

The theory has been applied to a particular configuration for which experimental pressure distributions are available. The correlation between theoretical and experimental surface pressures is favorable over the major part of the body; however, the theory fails to account for the large interference pressures near the wing-body junction and on the wing. The discrepancy is believed to be due to complicated shock boundary-layer interaction taking place near the corner, causing flow separation.

The theory predicts an optimum lift-drag ratio of about 5 for a typical wing-body configuration in a Mach 5 flow.

References

[1] Eggers, A. J., "Some consideration of aircraft configuration suitable for long-range hypersonic flight," Colston Symposium on Hypersonic Flow, Bristol, pp. 369–390 (1959).

[2] Migotsky, E. and Adams, G. J., "Some properties of wing and half-body arrangements at supersonic speeds," NACA RM A 57 E15 (1957).

[3] Savin, R. C., "Approximate solutions for the flow about a flat-top wing-body configuration at high supersonic air speeds," NACA RM A 58 FO2 (1958).

[4] Ferri, A., "The linearized characteristic method and its application to practical non-linear supersonic problems," NACA TN 2515 (1951).

[5] Cheng, H. K., "Hypersonic flow past circular cones and other pointed bodies," J. Fluid Mech. **12**, 169–191 (1962).

[6] Woods, B. A., "The flow close to the surface of a circular cone at incidence to a supersonic stream," Aeronaut. Quart. XIII, Part 2, 115–128 (May 1962).

[7] Willett, J. E., "Supersonic flow at the surface of a circular cone at angle of attack," J. Aerospace Sci. **27**, 907–912 (1960).

[8] Scheuing, R. A., "Outer inviscid hypersonic flow with attached shock waves," ARS J. **31**, 486–503 (1961).

[9] Fowell, L. R., "An exact theory of supersonic flow around a delta wing," Univ. of Toronto Institute of Aerophysics Rept. 31 (March 1955).

[10] Courant, R. and Friedrichs, K. O., *Supersonic Flow and Shock Waves* (Interscience Publishers, Inc., New York, 1948), Chap. 1A, p. 22.

[11] Mandl, P., "A theoretical study of the inviscid hypersonic flow about a flat-top wing-body combination," National Research Council, National Aeronautical Establishment Rept. LR-389 (1964).

[12] Stone, A. H., "On supersonic flow past a slightly yawing cone," J. Math. Phys. **27**, 67–81 (April 1948).

[13] Chernyi, G. G., *Introduction to Hypersonic Flow*, transl. by R. F. Probstein (Academic Press, New York, 1961), Chap. 3, p. 116.

[14] Holt, M., "A vortical singularity in conical flow," Quart. J. Mech. Appl. Math. **7**, 438–449 (1954).

[15] Hayes, D. and Probstein, R. F., *Hypersonic Flow Theory* (Academy Press, New York, 1959), Chap. 2.2, pp. 39–42.

[16] Milne-Thomson, L. M., *Theoretical Hydrodynamics* (The Macmillan Co., New York, 1955), 3rd ed., Chap. 20, pp. 584–585.

[17] Randall, R. E., Bell, R., and Burk, J. L., "Pressure distribution tests of several sharp leading edge wings, bodies, and body-wing combination at Mach 5 and 8," Arnold Engineering Development Center TN 60-173 (1960).

[18] Staff of the Computing Section, "Tables of supersonic flow around cones," Massachusetts Institute of Technology, Dept. of Electrical Engineering, Center of Analysis, TR 1 (1947).

[19] Ferri, A., "Supersonic flow around circular cones at angle of attack," NACA TN 2236 (1950).